Transmission Electron Microscopy Study of the Formation of FAU-Type Zeolite at Room Temperature

Valentin P. Valtchev*,† and Krassimir N. Bozhilov‡

Laboratoire de Matériaux Minéraux, UMR-7016 CNRS, ENSCMu, Université de Haute Alsace, 3, rue Alfred Werner, 68093 Mulhouse Cedex, France, and Central Facility for Advanced Microscopy and Microanalysis, University of California, Riverside, California 92521

Received: April 15, 2004; In Final Form: July 9, 2004

FAU-type zeolite was synthesized at room temperature to study the mechanism of its formation. The sluggish crystal growth kinetics at ambient conditions permitted us to track down the entire sequence of crystallization events from the formation of the initial gel to the complete transformation into a zeolite-type material. The processes taking place at the nanometer scale were studied by transmission electron microscopy (TEM). The crystalline character of the particles observed during the induction period was determined by in situ synchrotron XRD analysis. The study was completed by ex situ X-ray diffraction (XRD), infrared (IR), dynamic light scattering (DLS), N_2 adsorption measurements and chemical analyses. The combined TEM/synchrotron XRD analysis of the initial crystallization stage revealed that zeolite nuclei were formed during the homogenization (1.5 h) of the initial reactants. Nevertheless, a relatively long induction period (10 days) was observed. During this period, extensive exchange between the solid and liquid parts of the system took place. However, the changes in the chemical composition of the gel and mother liquor were not coupled with a detectible increase of the number of nuclei. It seems that the critical factor that triggers the growth process and mass transformation of amorphous into crystalline zeolite material is the attainment of a specific level of chemical evolution of the system, expressed in homogenization of the starting gel approaching stoichiometric FAU compositon. The process of zeolite formation can be divided into four general stages: (i) 0−1.5 h, formation of an amorphous gel with highly variable composition, local formation of stable zeolite nuclei, and nanometer sized metastable hydrated silica phase; (ii) 1.5 h to 10 days, chemical evolution of the gel composition that is coupled with structural rearrangements of the amorphous gel and further development of zeolite nuclei; (iii) 10−14 days, spontaneous mass transformation of the amorphous gel into spherical aggregates of small (10−20 nm) crystals around individual crystallization centers of viable nuclei and collapse of the metastable phases; (iv) 17−38 days, crystal growth involving agglomeration, dissolution, and regrowth of individual nanoparticles around spherical aggregates.

Introduction

Aluminosilicate zeolites constitute a family of crystalline solids with open-framework structures. The continuing efforts to synthesize new materials in this class and to improve our understanding of their crystallization mechanisms, is driven by the broad range of useful and unique properties they possess. Zeolites contain uniformly sized pores in the range of 3−10 Å and can thus display molecular recognition, discrimination, and organization properties with a resolution of less that 1 Å. These characteristics are the basis for their immense importance in catalysis, separations, and ion exchange.[1]

Nowadays, the discovery of new zeolites is still a mainly heuristic exercise involving systematic exploration of many reaction variables, and requiring a fair degree of serendipity for the successful synthesis of new materials.[2] Because the events in the early stages are of critical importance in determining the course of the subsequent crystallization, it is clear that a detailed understanding of these phenomena should be obtained if the goal of a rational control of the synthesis of these materials is to be achieved. Aluminosilicate zeolites are synthesized under hydrothermal conditions where the reaction variables include time, temperature, pressure, gel composition, the inorganic and organic cations used, reactant source and type, pH, aging time of the gel, reaction cell fill volume, and so on.[3] The effect of varying one of these parameters is difficult to evaluate in a straightforward manner, because it may have an effect on several others. The reaction system is in general inhomogeneous with both liquid and solid components, thus zeolite nucleation and crystal growth involve numerous simultaneous equilibria and condensation steps,[4] which further complicates the analysis and interpretation of the crystallization process.

Usually, the studies of the zeolite nucleation and growth mechanisms are based on characterization of the precursor amorphous suspensions and crystalline particles by ex situ methods such as X-ray diffraction, SEM, IR/Raman and NMR spectroscopy, etc. The structure of the small unstable colloidal particles existing in the precursors could be altered if an invasive postsynthesis sampling procedure is applied. Sample modifications may include redistribution of (alumino)silicate species, particle growth, and possible initiation of nucleation. Very often these changes complicate the interpretation and lead to erroneous conclusions. Substantial progress in the understanding of zeolite

* Corresponding author. E-mail: V.Valtchev@uha.fr. Fax: (33) 03 89 33 68 85.
† Université de Haute Alsace.
‡ University of California.

10.1021/jp048341c CCC: $27.50
Published on Web 09/11/2004

formation has been achieved by application of in situ characterization techniques such as NMR,[5,6] IR/Raman,[7] EXAFS,[8] optical and electron microscopy,[9] light-scattering techniques,[10−12] X-ray diffraction,[13−15] and combinations of SAXS/SANS[16,17] and SAXS/WAXS.[18,19] These in situ characterization methods convey more truthful insight into the process of zeolite formation. However, they do not provide specific and localized information about the transformation of amorphous colloidal particles into crystalline matter. In addition, the in situ studies of zeolite formation are far from routine procedure and impose considerable technical constraints. The main difficulty is the necessity of constructing reaction cells that are able to withstand the relatively high temperatures and pressures required for the synthesis of zeolites. The cell is usually small and the heterogeneous reactions taking place on the walls have greater impact on zeolite formation than in conventional autoclaves.

Generally, the studies on zeolite formation have been performed at elevated temperatures without taking into account the events taking place in the gel at low temperature. It is well-known, however, that the aluminosilicate zeolites may crystallize under ambient conditions. Indeed, natural zeolites are often formed at low temperature in closed alkaline and saline-lake systems.[20] LTA-type zeolite with crystallinity of about 75% was obtained after 30 days at room temperature.[21] There are numerous proofs that the events taking place in the gel phase under ambient conditions are of primary importance for the subsequent crystallization process. For example, the aging of gels yielding zeolite Y suppresses the formation of other zeolite phases and decreases the crystallization time.[22,23] Several groups have suggested that the aging step results in the formation of viable nuclei, which induce the crystallization when the temperature is raised.[3,24,25] Subotic et al.[26,27] developed the "autocatalytic nucleation" model in which nuclei liberated during the dissolution of the gel phase promote zeolite crystallization. Further development of this model revealed that it can be applied successfully only to nuclei that are located near the outer surface of the gel particles.[28,29] The localization of the viable zeolite nuclei, which promote crystallization, is an important issue that could shed light on subsequent events in the process of zeolite crystallization.

As it was discussed above, zeolite formation is still not well understood, except in that it appears that there is no single universal mechanism to describe all zeolite syntheses. The two extremes of the proposed mechanisms of zeolite formation are (i) solution-mediated transport mechanism[30] and (ii) solid hydrogel transformation mechanism.[31] In any particular reaction system the true mechanism could lie somewhere between these two extremes.[4,32,33] Lately, AFM investigations showed that several zeolite materials grow by the layer mechanism.[34,35] Very little is known, however, about the nucleation and crystal growth processes during the initial few hours of the crystallization of even the simplest zeolites. Moreover, the nucleation of zeolites seems to be contrary to the classical nucleation theory,[32,36] according to which the nucleation occurs in the liquid phase. The simultaneous SAXS/WAXS observations have revealed that the nucleation occurs inside the amorphous gel.[18,19] Direct observation of such a nucleation mechanism was performed by a TEM investigation of the formation of TMA-LTA-type zeolite under ambient conditions.[37] Although it is now generally accepted that the nucleation takes place in the gel phase, it is not a proven fact for each specific zeolite system. In regard to this, the characterization of the nucleation process of any particular zeolite requires the following two important questions to be answered: (i) where does the nucleation take place in the liquid or in the gel phase and (ii) which stage of the gel reorganization are the viable nuclei formed at.

In the present study we conducted the experiments at room temperature, to study the events during the nucleation stage of FAU-type zeolite with minimum invasive postsynthesis treatments. The slow crystal growth kinetics at room temperature allowed us to discriminate different stages of the zeolite formation and to understand better the effect of aging. The study was based mainly on transmission electron microscopy (TEM), which is a method for direct localized structural studies at unit cell level. Complementary investigations were performed to obtain more comprehensive information on the mechanism of zeolite formation.

Experimental Section

Synthesis. To obtain FAU-type zeolite in a reasonable period of time under ambient conditions, a very reactive system was employed. A silica source containing low-mass silica species was used and further depolymerized by adding sodium hydroxide so as to obtain a completely transparent initial solution. The latter was mixed with a clear aluminate solution where $Al(OH)_4^-$ is the dominant anionic species.[3] The zeolite precursor mixture was produced by vigorous mixing of the alkaline silicate and aluminate solutions, prepared as described above, where all components were expected to be relatively homogeneously distributed. The composition of the gel was as follows: $4Na_2O$:$0.2Al_2O_3$:$1.0SiO_2$:$200H_2O$. The reactants used for the preparation of the gel were sodium hydroxide pellets (97%, (Aldrich), sodium aluminate (54.3% Al_2O_3, 44.5% Na_2O, Riedel-de Haën), sodium silicate solution (14% NaOH, 27% SiO_2, Fluka), and distilled water. The mixture kept its transparent character for several seconds and after that transformed to a milky-white low-viscosity gel. The initial mixture was stirred for 1.5 h and transferred in a polypropylene bottle. The sealed bottle was stored in an oil bath ($T = 25 \pm 1$ °C). One hour later a thin layer of clear solution was observed in the upper part of the reaction vessel. The milky-white color and the observed sedimentation revealed that the gel comprised relatively large particles. Small aliquots of the mixture were taken at different periods of time. Prior to taking aliquots the sample was shaken to disperse settled particles. During the first day three samples were taken, immediately after homogenization of the gel (1.5 h), after 6 and 24 h. After the first 24 h, further samples were taken every 2−3 days. The solids were recovered by high-speed centrifugation ($g = 50\,000$) and redispersion in distilled water under ultrasonic radiation. Part of each solid was dried at room temperature and the other part was kept as a suspension.

FAU-type samples prepared under ambient conditions were compared to a sample synthesized at 95 °C for 5 h, after 24 h aging at room temperature. The sample was recovered by suction filtration and dried overnight at 60 °C.

Characterization. The structural evolution of the gel species was tracked down with high-resolution transmission electron microscopy (HRTEM), in a FEI-Philips CM300 microscope in low-dose mode operating at 300 kV accelerating voltage, equipped with a LaB_6 electron gun, and EDAX energy-dispersive X-ray spectrometer (EDS). Samples were prepared by diluting the suspension of the reaction products in distilled water, ultrasonicating them, and depositing a drop onto Cu grids coated with a thin (5 nm thickness) holey carbon support film. To verify that the zeolite crystals do not collapse under the high vacuum in the TEM, some of the samples were studied at liquid nitrogen temperature using a Gatan Inc. cryo-system, model 626. No apparent increase in crystallinity or size distribution was

observed, which allowed us to conclude that utilization of a low-dose technique at room temperature is an adequate method for characterization.

The compositions of synthesis products were determined quantitatively in the TEM, by localized EDS analysis of areas from 20 to 300 nm in diameter, utilizing experimentally determined *k*-factors and following the procedure described by Bozhilov et al.[38]

The in situ powder diffraction study of the sample aged for 4 days was performed by synchrotron X-ray radiation (λ = 0.8 Å) at ESRF-Grenoble (beamline ID01). The experiment was performed in a specially designed reactor made of stainless steel with Teflon windows. The size of the beam was 1.0 × 0.5 mm. The measurement was carried out in the transition mode by using a linear position sensitive detector with an energy of 15.5 keV.

To complement these studies, X-ray diffraction (XRD), dynamic light scattering (DLS), IR spectroscopy, and N_2 adsorption measurements were performed. The XRD diagrams of the samples were recorded on a STOE STADI-P diffractometer in Debye−Scherrer geometry equipped with a linear position-sensitive detector (6° in 2θ) and employing Ge monochromated Cu Kα_1 radiation. The particle size analysis was performed with a dynamic light scattering instrument (Malvern, HPPS-ET). Prior to analysis the samples were diluted with distilled water. Electron micrographs were taken on a Philips XL30 LaB_6 scanning electron microscope (SEM). IR analyses were performed on samples pressed in KBr with a Perkin-Elmer PE−2000 FTIR spectrometer. Nitrogen adsorption measurements were carried out with a Micromeritics ASAP 2010 surface area analyzer. The samples were outgassed at 345 °C overnight prior to analysis. The specific surface areas were calculated with the BET equation. A pure highly crystalline FAU-type sample synthesized from a similar gel with a BET specific surface area (S_{BET}) of 613 m^2/g was used as a reference.

The elemental analyses of the solids were performed on an X-ray fluorescence spectrometer MagiX (Philips). Prior to the analysis the powdery sample was melted with $Li_2B_4O_7$ at 1300 °C. The resultant glass bead was analyzed under vacuum with a Rhodium anticathode (2.4 kW). The mother liquor separated by high-speed centrifugation from the solid was analyzed by atomic absorption spectroscopy (Varian Techtron AA6).

Results

General Characterization of the Samples. The ex situ XRD study did not show any crystallinity of the material with synthesis duration less than 11 days. A small peak corresponding to d = 14.3 Å, which is the most intense reflection in the XRD pattern of the FAU-type materials, was detected after 11 days. The amount of the crystalline phase is close to the detection limit of the XRD technique, which is in the order of 3−4 wt % FAU-type material (Figure 1a). Between day 11 and 22 of the synthesis the crystallinity increased gradually (Figure 1b,d). According to the XRD study, further room-temperature synthesis did not increase the crystallinity of the FAU-type zeolite (Figure 1e). Even for the most crystalline samples, the XRD peaks were relatively broad, indicating the presence of very small zeolite particles. Other crystalline phases were not detected. The halo in the XRD patterns revealed the presence of amorphous material in the products, which decreased with time.

The crystalline nature of some of the samples was studied by in situ synchrotron XRD. After homogenization of the initial reactants, the sample was placed in a specially designed reactor and kept at 25 °C for 4 days. After 4 days, the initial mixture comprised two parts: an upper part where a clear solution free of gel particles was observed and a lower part where the gel phase had sedimented. The high-intensity X-ray beam allowed us to record Bragg reflections in the gel part, next to the interface with the clear solution. Thus, the most intense peak at 2Θ = 3.29° corresponding to d = 14.3 Å, which is reflection from the {111} planes in FAU-type material is clearly seen in Figure 2, whereas the other reflections were not detected. The synchrotron XRD investigation of the liquid over the gel phase did not detect any crystalline material. A complementary IR study was performed on a series of samples synthesized at room temperature between 1 and 32 days (Figure 3). The samples synthesized for 1−10 days show broad absorption bands in the range 400−1200 cm^{-1}, which are typical of amorphous sodium aluminosilicate gels.[39] Structure sensitive vibrations of the faujasite structure are near 555, 665, and 745 cm^{-1}. It was difficult to distinguish these bands, even in the sample showing the presence of XRD crystalline material (11 days). However, the IR bands indicative of the formation of the zeolite structure can be clearly seen in the spectrum of the material after 2 weeks. The samples synthesized for more than 2 weeks possess well established and distinct structural bands, which become sharper

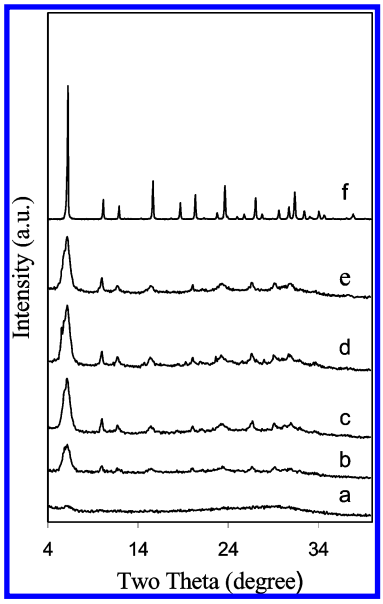

Figure 1. Evolution of the crystallinity of FAU-type zeolite under ambient conditions according to the XRD analyses: (a) 11 days; (b) 14 days; (c) 18 days; (d) 22 days; (e) 32 days; compared with the reference sample synthesized at 90 °C (f).

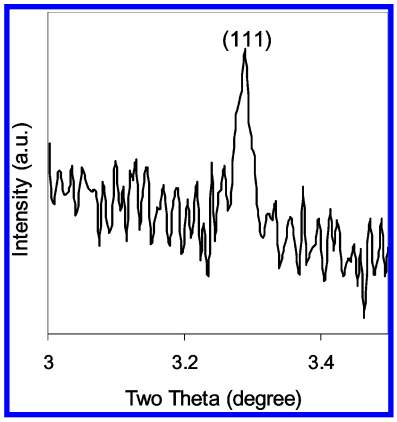

Figure 2. (111) reflection of zeolite X recorded by in situ synchrotron XRD in the solid part of the gel aged at 25 °C for 4 days (λ = 0.8 Å).

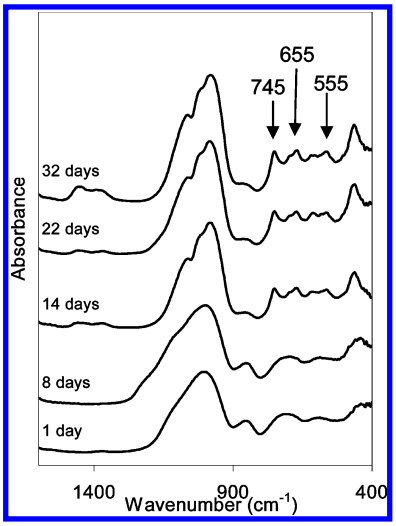

Figure 3. IR spectra of the reaction products from a series of experiments with synthesis durations extending from 1 to 30 days. The IR absorption bands characteristic for the FAU-type structure (555, 665, and 745 cm^{-1}) are well distinguished after 2 weeks hydrothermal treatment.

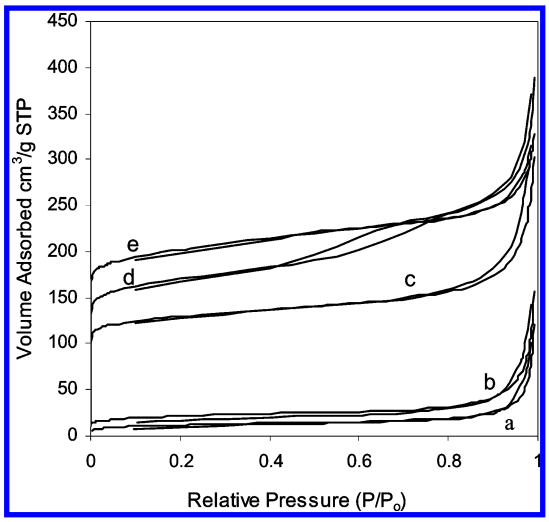

Figure 4. Adsorption/desorption isotherms of the samples obtained after 3 (a), 8 (b), 14 (c), 26 (d), and 32 (e) days hydrothermal treatment under ambient conditions. A substantial increase of the microporosity can be observed after 14 days synthesis.

with increasing synthesis time. The increase of the intensity of the structure sensitive bands is accompanied by a decrease of the band at about 850 cm^{-1}. The gradual decrease of this band, assigned to a Si−OH bending vibrations, suggests that the number of framework atoms connected via oxygen bridges increases with time.

The adsorption isotherm (type I) and the specific surface area are important characteristics of microporous materials. The adsorption/desorption isotherms of the samples obtained after 3, 8, 14, 26, and 32 days are shown in Figure 4. A steep rise in the uptake, followed by a flat curve at low relative pressures, corresponds to filling of micropores with N_2. As can be seen, the samples synthesized for 3 and 8 days do not possess open micropores, whereas the other three synthesized for 14, 26, and 32 days comprise substantial microporous volume (Figure 4). At high relative pressures another upward turn can be seen, which is indicative of filling of the inter particle spaces. The BET specific surface areas of the samples are presented in Table 1. There is only a slight difference in the N_2 adsorption data for the samples taken after 1 and to 8 days synthesis (Figure 4a,b). A substantial increase was observed after 14 days. In the period 14−32 days, the specific surface area of the solid progressively increased and reached almost 600 m^2/g. This value equals that of the highly crystalline reference sample synthesized at 95 °C from a similar initial gel. It is worthwhile to mention that the increase of the surface area after 3 weeks synthesis at room temperature was negligible, but still indicative for the continuing evolution of the system. Although the increase of the specific surface area was not accompanied by visible changes in the XRD patterns of the samples taken after 22 days, the most probable explanation of such discrepancy is the increased crystallinity of the material.

TABLE 1: BET Specific Surface Areas of the Solids Obtained under Ambient Conditions

synthesis time (day)	0.06[a]	1	3	4	8	14	21	26	32
BET surface area (m^2/g)	35	47	63	59	74	434	521	574	598

[a] Sample taken immediately after the homogenization of the gel.

There is good agreement between XRD, IR, and N_2 adsorption data that the relatively long induction period is followed by a progressive transformation of the amorphous phase into a crystalline FAU-type material. According to these data the induction period lasted about 10 days under ambient conditions. First indication of crystallinity was detected by XRD after 11 days and the mass transformation of the amorphous material into a crystalline FAU-type structure started after about 14 days synthesis at room temperature and was almost completely crystalline after 17 days. The XRD crystallinity continued to increase slowly to 21 days, whereas after that, only the BET specific surface area measurements showed slight increase of the total S_{BET}, which was attributed to continuing zeolite growth. The increase of the BET surface area of the samples synthesized for 26 and 32 days is not necessarily connected with an increase in the zeolite crystallinity. It may be also due to dissolution of low surface area amorphous material.

TEM Investigation. The evolution of the system was studied by TEM to investigate the intimate steps during the transformation from amorphous to crystalline material and to identify the events taking place during the formation of the FAU-type zeolite. After thorough mixing of the initial reactants large nonuniform gel particles were formed (Figure 5a). The detailed TEM study of this gel showed that its structure was not homogeneous. At high magnifications it can be seen that the structure of the gel is grainlike, containing particles with sizes ranging between 10 and 50 nm. The grainlike appearance of the gel phase is due also to the presence of brighter, relatively isometric areas, which were almost homogeneously distributed in the volume of the gel particles (Figure 5b−d). The difference in the contrasts in the bright-field (BF) imaging mode is indicative of the presence of material with composition of lower average atomic number (*Z* contrast). The EDS analyses of such particles revealed that they do not contain Al, or if present, it is in trace amounts (Figure 5b). On the basis of the diffraction contrast differences, and the EDS analyses, the darker areas can be attributed to the part of the gel rich in aluminosilicate species, whereas the bright spots correspond most probably to a highly hydrated silica phase or silica-rich liquid inclusions trapped in the amorphous mass. This kind of specific structure of the gel is observed in the sample taken immediately after the homogenization (Figure 5c). The silica inclusions or brighter spots were observed in all experiments during the first 10−12 days. They disappeared together with the large nonuniform aggregates, i.e., during the mass transformation of the amorphous precursor into crystalline FAU-type material. It is worth mentioning that the outlines of some of the silica-rich bright spots are straight and

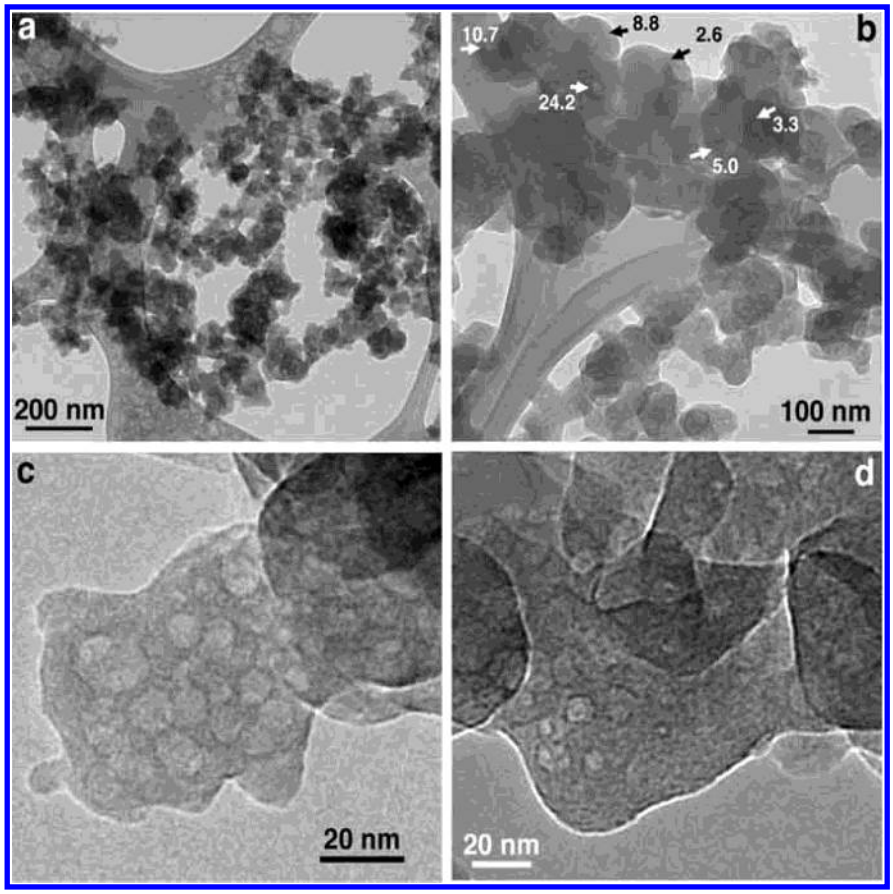

Figure 5. TEM micrographs showing the structure of the gel material during the initial stages of formation: after 90 min (a, c), 15 h (b), and 12 days (d). In (b) are shown the locations of individual EDS spot analyses (marked by arrows), and next to each location the corresponding Si/Al ratio is given. The gel is compositionally inhomogeneous. Note the difference in appearance between the lower and upper part of (b) due to the disappearance of the grainy structure of the upper part, which was exposed for a longer time under the focused electron beam. The faceted shape of the bright areas can be seen in (c) and (d), suggesting crystalline nature of these particles (see text for further details).

faceted, resembling crystal faces (Figure 5d). It is possible that these are crystalline forms of highly hydrated silica or negative crystals starting to form from a liquid inclusions trapped in the gel. Negative crystals are faceted cavities inside solid material or crystal filled with mother medium, which could be in the form of solution or gas.[40−44] The faceted shapes are a clear indication of the presence of ordered structure at the interface or indicate that these inclusions were crystals containing highly hydrated species, which collapse in the vacuum of the TEM. As a consequence of such instability, no electron diffraction or lattice contrast could be obtained from such areas.

To visualize possible crystalline phases, we used dark-field (DF) imaging. All samples taken between 1 and 10 days were systematically studied. The DF images revealed that there are crystals present in all samples with different synthesis duration. According to the TEM analysis all samples from synthesis duration less than 10 days contained an approximately equal number of crystalline particles. In other words, the reorganization of the gel phase during the induction period did not result in particles with distinctive crystalline features that can be detected by means of TEM. The sample taken immediately after the homogenization procedure (Figure 6a,b) contained crystalline particles whose number and distribution was similar to those of 7 days synthesis (Figure 6c,d). The DF imaging was done on areas of $1-4\ \mu m^2$. For each sample total area of about 100 μm^2 was analyzed. The average number of crystalline particles per square micron of gel area is around 75 with standard deviation of 16.5. No trend of increase or decrease with time was observed, and the average value for each run was within the standard deviation of the total average. This result clearly shows that crystalline particles were formed during the process of stirring of the initial reactants, and there is no positive evidence that they have zeolite composition or structure. An increase of the number of the crystalline particles with synthesis time can be expected, if they were formed during gel aging, but such an increase could not be confirmed by our observations. The nonzeolite crystals are most probably nonequilibrium sodium silicate/aluminate phases. No other crystalline material except zeolite was detected in the final product, which suggests that the nonequilibrium phase(s) disappeared during the mass transformation of the aluminosilicate species into a FAU-type material.

Selected area electron diffraction (SAED) patterns from all samples with synthesis duration less than 12 days contain discrete spot reflections (Figure 6c inset), which are not consistent with the FAU-type structure. These reflections have been attributed to a metastable Na-silicate/aluminate phase of unknown structure, which disappears in the final stages of synthesis. The SAED patterns from 4 to 12 days synthesis duration contain also diffuse rings corresponding to *d* spacings of 4.8 and 2.7Å, which can be attributed to the {333} and {555} reflections from nuclei with the FAU-type structure. The presence of the (111) reflections (14.2 Å) could not be confirmed or excluded due to the strong scattering of the amorphous material close to the transmitted spot.

HRTEM imaging did not bring many more direct clues about the location of the crystalline FAU-type nuclei from the initial 10 days of synthesis. The failure to obtain structural images is

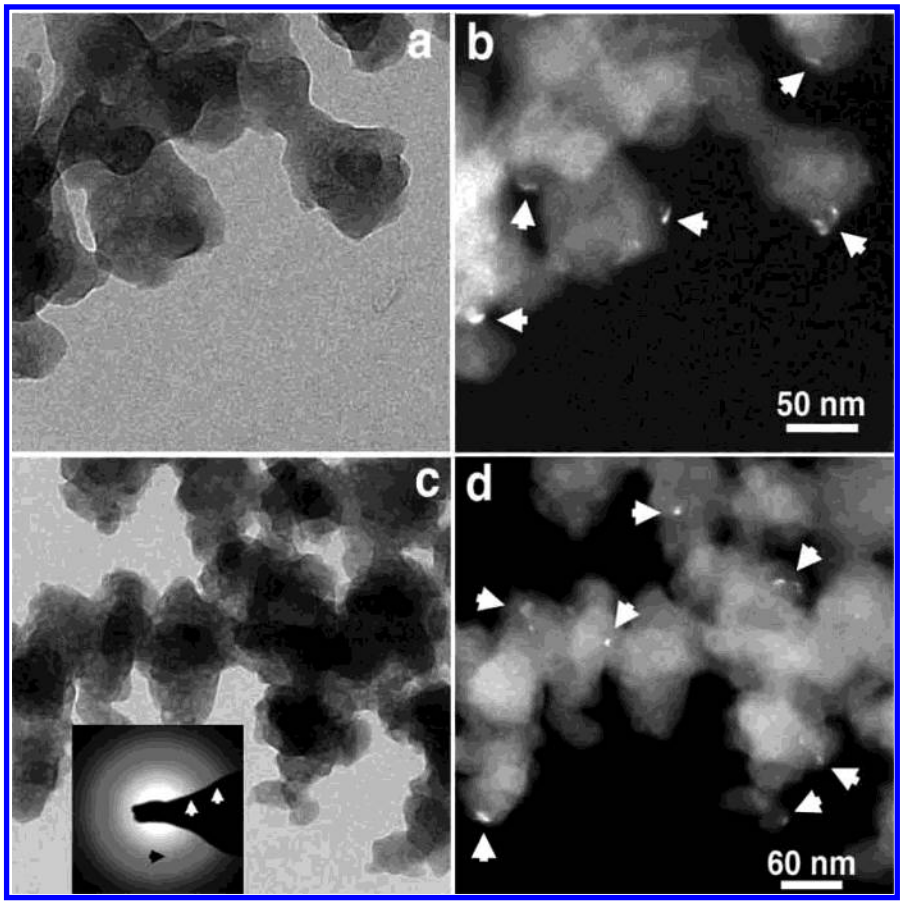

Figure 6. Pairs of BF/DF images obtained in the TEM from the synthesis products after 90 min (a, b) and 7 days (c, d) of treatment. The crystalline particles are marked by white arrows in the DF images. As an inset in (c) is shown a SAED pattern obtained from the synthesis products after 7 days. The two diffuse rings (marked by white arrows) correspond to *d* spacings of 4.8 and 2.7 Å respectively, which are consistent with the {333} and {555} reflections of the FAU-type structure. A black arrow points to a single spot reflection corresponding to *d* spacing of 3.5 Å and is attributed to the Na-silicate/aluminate crystalline particles with unknown structure which are visualized in DF mode.

caused most probably by two factors. First, it is possible that these nuclei are extremely beam sensitive and undergo complete amorphization under the high current density of the focused electron beam necessary to form HRTEM images. The second possibility is that they are fully embedded in the amorphous gel and do not produce detectable contrast in the TEM. Because HRTEM images of the FAU-type crystals were obtained relatively easily from the crystalline product from long synthesis duration, it can be concluded that the stability of the zeolite is not the limiting factor. HRTEM observations combined with the SAED data suggest that most probably the nuclei formed in the beginning stage are completely surrounded by amorphous material, which prevents their visualization.

The presence of negative crystals and liquid filled voids can be regarded as one of the potential locations initiating zeolite nucleation. The gel−liquid interface, where an extensive exchange between the solid and liquid part of the system takes place, is a very likely place for the zeolite nucleation to occur. Such a hypothesis is in agreement with the analysis of Tsapatsis and co-workers,[45] who showed that gel microstructure plays an important role in zeolite nucleation by defining the interfacial area between the gel and the solution.

After 12 days synthesis large gel aggregates were still observed (Figure 7a). Some of them comprised particles with well-defined crystal structure, which allowed lattice fringes to be obtained by HRTEM, whereas others were completely amorphous. The appearance of the amorphous and crystalline aggregates is similar; however, the crystalline product is easily distinguishable by the 14 Å lattice spacing attributed to the {111} planes of the FAU-type structure (Figure 7, inset). The area where the crystalline fringes were observed is about 30 nm^2. It is worthwhile to mention that the crystalline area retains the grainlike morphology of the gel phase (Figure 5a,b) and many of these grains were included in the FAU-type crystals.

This is sound evidence that the crystallization process at this early stage takes place via propagation through the amorphous network. This growth mechanism was rapidly substituted or takes place simultaneously with a process of aggregation of particles around a crystallization center. The TEM micrograph of the material obtained after 14 days, where still a substantial amount of amorphous material is present, showed that isometric crystalline aggregates with a diameter of about 100 nm already exist in the system (Figure 7b). However, the crystalline aggregates are still embedded in the amorphous matrix at this stage.

Although the ex situ XRD analysis did not detect any increase of the crystallinity after the samples have aged for more than 3 weeks crystallization, the TEM investigation showed substantial changes in the size and morphology of the particles building up the aggregates. The aggregates formed after 17 days are 100−300 nm in size, and some of them consist of crystalline particles of two different size populations, the first one represents small 10−20 nm size crystals and the second consists of crystals longer than 50 nm in size (Figure 8a,b). The small crystals predominate in quantity and they are located in the middle of the aggregates whereas the large ones are in the periphery. After 3 weeks or longer synthesis times, the number of the small crystals decreases and the aggregates are built up from crystals

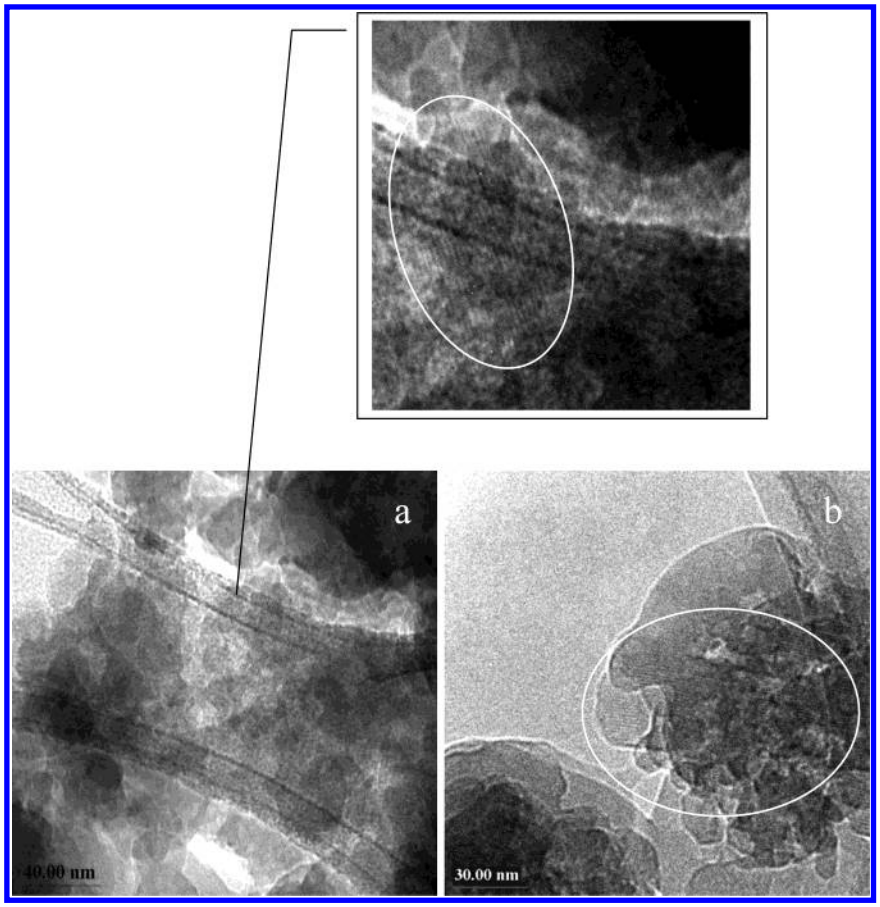

Figure 7. TEM micrographs of the product synthesized for 12 (a) and 14 (b) days of crystallization at room temperature. The crystalline areas are marked with white contour lines. The inset of (a) shows the lattice fringes spread over the grainlike particles.

of similar size (Figure 8c,d). The prolongation of the synthesis duration to 32 and 38 days did not change the ultimate size of the aggregates (Figure 8c,e). However, the size and the morphological features of the particles building the aggregates changed substantially. The crystals, especially in the peripheral part of the aggregates, became bigger with distinctive crystal morphology (Figure 8d). After 38 days crystallization, crystals with a size up to 100 nm were observed, and the octahedral morphology typical for the FAU-type zeolite can be seen (Figure 8f). The significant observation is that the presence of small crystals is substantially reduced compared to the syntheses less than 3 weeks long. Because the system at this stage did not contain amorphous material, which can serve as a nutrient pool, the observed growth of the particles can be attributed to the dissolution and regrowth of a part of the crystals.

DLS Investigation. The DLS measurements were consistent with the TEM investigation. During the first 10 days of the synthesis large particles exceeding 10 μm were the dominant population. Further aging resulted in the formation of particles with sizes below 1 μm. Thus, after 12 days at room temperature two distinct populations of particles with mean radii of about 750 and 150 nm were observed (Figure 9), which correspond most likely to the particle aggregates observed in the TEM. Together with these two particle classes, still larger particles were observed in the sample. After 3 weeks under ambient conditions, the very large gel particles as well as the population of 750 nm completely disappeared. The particles with a mean radius of about 150 nm became the dominant fraction and a small fraction of particles with a radius of about 25 nm was also present in the product.

Discussion

The formation of FAU-type zeolite at room temperature corresponds to the nucleation/crystallization mechanism observed at elevated temperatures, where the nucleation and crystallization events are generally illustrated by characteristic S-shaped crystallization curves. After a relatively long induction period (11 days), the first crystalline matter was detected and the mass transformation of the amorphous into crystalline FAU-type material was observed between 14 and 17 days of synthesis at room temperature. The crystallization was completed in 22 days. These observations can be considered in light of the so-called autocatalytic nucleation,[26−29] where the nuclei become active only after they are released into solution. Due to the crystal growth of liberated nuclei, the zeolite surface area increases, which accelerates the reaction rate. To get an insight in the nucleation process, a detailed TEM investigation was performed on samples taken during the induction period.

The detailed TEM study showed that the gel structure is predominantly amorphous initially. The EDS analyses in the TEM at nanometer scale demonstrated that the gel is highly inhomogeneous at the start of the process and slowly attains chemical homogeneity in about 2 weeks (Table 2). The amorphous aggregates formed in the beginning have very complex morphology with many branches and cavities. They consist of individual amorphous particles in the range of 10−50 nm diameter that are in close contact with each other and form the complex structure of the aggregates with large surface area in contact with the liquid. In addition, the gel is not homogeneous structurally, it contains voids filled most probably with liquid

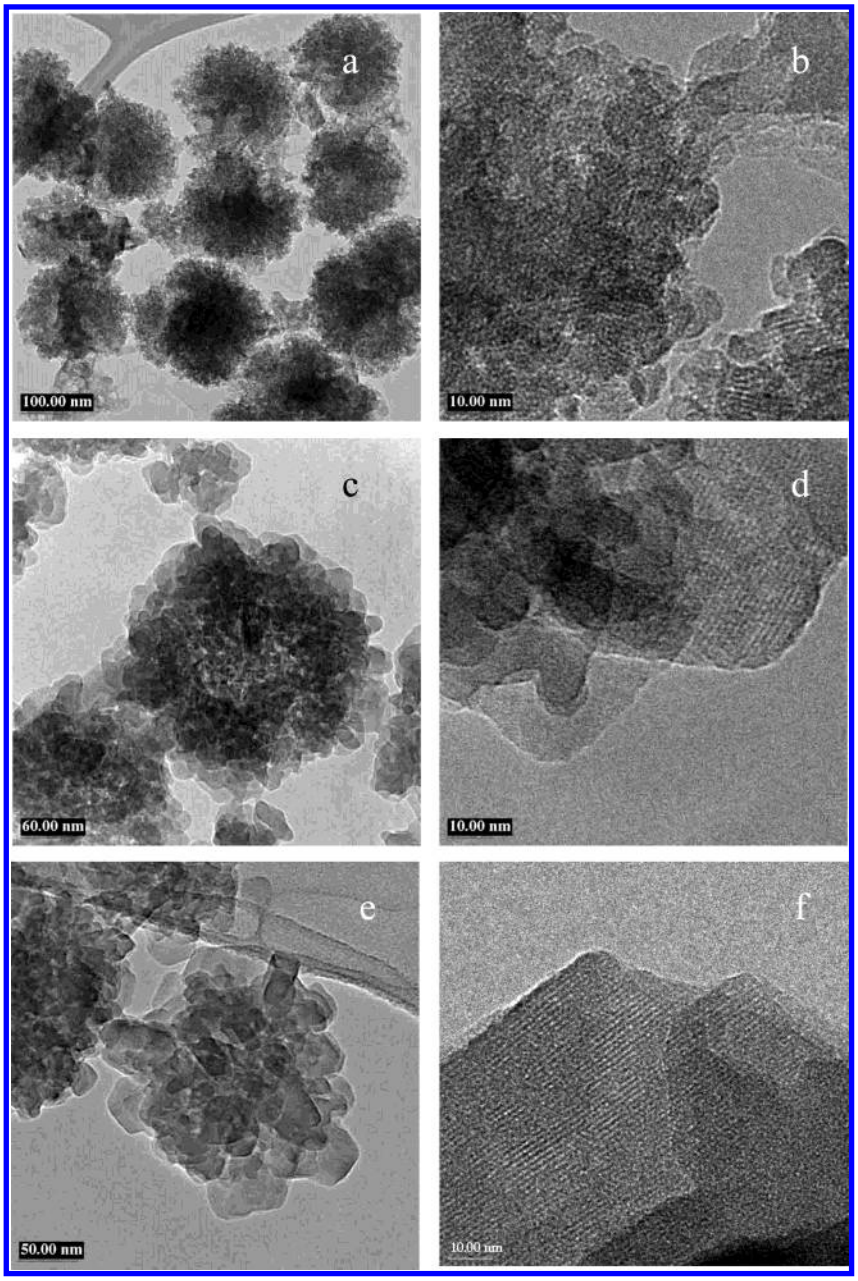

Figure 8. TEM micrographs of particle morphology and crystal lattice for samples aged more than 3 weeks: 17 days (a, b); 22 days (c, d); 38 days (e, f).

TABLE 2: Si/Al Ratio for Three Different Experimental Materials Obtained by EDS Analysis in the TEM

synthesis time	15 h	12 days	17 days
average Si/Al	6.41	4.11	1.46
median Si/Al	2.19	1.69	1.30
standard deviation	9.47	4.98	0.09
number of analyses	27	26	29

phase as well as abundant crystalline particles of hydrated silica, which are between 5 and 15 nm in size and are randomly distributed.

On the basis of the both the SAED patterns and in situ synchrotron XRD, it is evident that FAU-type nuclei are present in the gel mass for experiments with duration of 4−10 days. No direct visualization of the nuclei by HRTEM was possible, but on the basis of the size and structure of the gel aggregates, it can be stated that there are no parts in this initial gel that are situated topologically more than 50 nm from the liquid phase. According to the revised model of the autocatalytic nucleation, the dormant nuclei should be located near the surface of the

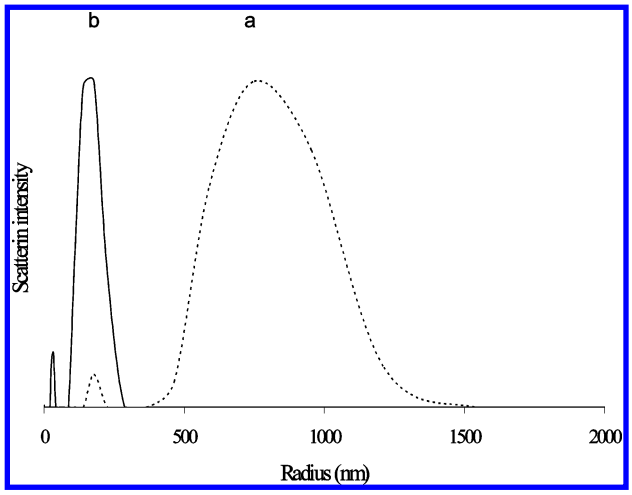

Figure 9. DLS data of suspensions obtained after purification of the samples synthesized for 12 (a) and 21 (b) days.

TABLE 3: Si/Al Ratio in the Solids Obtained by X-ray Fluorescence Spectroscopy after Different Periods of Time under Ambient Conditions

synthesis time (day)	1	9	14	22	32
Si/Al in the solid	1.35	1.32	1.21	1.19	1.20

gel particles.[29] Due to the complex structure of the gel aggregates that possess a fairly complicated "open" morphology, terms such as internal and outer surface of the gel become very relative and not very precise.

The presence of crystalline nonzeolite particles, imbedded in the abundant amorphous phase does not seem to have direct relation to zeolite nucleation. Although difficult to prove, a possibility exists that the presence of relatively stable silica phase acts as an inhibitor of the zeolite nucleation because it arrests the process of chemical homogenization of the gel and slows down the attainment of the appropriate Si:Al ratio which favors zeolite formation.

The DF imaging in the TEM shows that the number of crystalline particles does not increase during the first 10 days of synthesis. We reckon that these observations are statistically valid because the heterogeneity of the samples is on a nanometer scale level, whereas on the millimeter scale level the samples are homogeneous. However, if there is some dominance of the nucleation rate versus the dissolution rate during this period, it seems to be limited.

It was confirmed by the synchrotron in situ XRD study that crystalline FAU-type material is present in the beginning stage. This information combined with the electron diffraction data and TEM observations leads us to the conclusion that the zeolite nuclei form inside the amorphous gel particles. Such interpretation is supported by the fact that despite the very thorough and systematic TEM study of the gels no individual crystallites of newly formed zeolite could be observed. We were able to establish by the study of the control samples that FAU crystals are sufficiently stable in the TEM, which permitted lattice images to be obtained without difficulty. Both facts, namely the identification of FAU crystals by synchrotron in situ XRD and electron diffraction and the lack of clearly identifiable crystal by HRTEM imaging, suggest that the crystallites of the zeolite nuclei form inside the gel particles. Such a structure where small crystals are completely surrounded by an amorphous mass prevents us from obtaining lattice images by HRTEM because of absorption and scattering of the phase contrast signal originating from the small crystalline inclusions. This observation is consistent and indirectly supports the interpretation of nucleation inside the gel phase.

Thus, from these findings it can be concluded that (i) the induction period extends for about 10 days, during which period a chemical reorganization of the gel takes place, and (ii) the nuclei of the FAU-type material form inside in the gel phase.

Evidence for the chemical evolution of the system was provided also by analyses of the solid and liquid parts of the system. The solid was separated from the solution via high-speed centrifugation and analyzed by X-ray fluorescence spectroscopy. The changes in the Si/Al ratio in the solids obtained for different synthesis duration at room temperature are given in Table 3. There is no substantial difference between the Si/Al ratio of the solid after 1 and 9 days. A decrease of the ratio was observed after 14 days, which is the stage of mass transformation of the amorphous into crystalline material. No significant changes in the Si/Al ratio of the solid were observed after that stage. The Si/Al ratio of the final product corresponds to a zeolite X-type material, although the composition of the gel was designed for the preparation of zeolite Y. It is well-known that the cores of FAU-type crystals are Al-rich and in the course of the crystal growth the concentration of silicon increases.[23] Therefore, the formation of FAU-nanocrystals under ambient conditions with a composition corresponding to zeolite X is not surprising.

There are substantial fluctuations in the silicon content in the supernatant (Figure 10). In the period 1−9 days the silicon content in the solution increased, which is obviously due to depolymerization of the silica (Figure 10a). A relatively sharp decrease was observed in the period 9−14 days, which corresponds to the onset of the crystallization and mass transformation of the amorphous into a crystalline zeolite material. After this period the silicon content in the supernatant is almost constant. Furthermore, a direct correlation between the aluminum content and the crystallinity of the solid was found. The aluminum content in the mother solution decreased gradually and was almost totally exhausted after 14 days room-temperature synthesis (Figure 10b). In contrast to the aluminum, the concentration of sodium increased in the course of zeolite crystallization (Figure 10c). After the formation of the zeolite framework, the overall negative charge is substantially reduced with respect to that of the amorphous solid, which explains the decrease of sodium in the crystalline product. According to the XRD analysis after 14 days the amorphous material was still largely present in the system (Figure 7). Nevertheless, the composition of the amorphous phase was similar to that of the crystalline product. These data clearly show that the system reaches a specific critical level of chemical evolution before the onset of crystallization. Under "specific level of chemical evolution" we understand the stage when the solid reaches a composition corresponding to the composition of the zeolite material and the supernatant is in dynamic equilibrium with the solid part of the system. It is reasonable to assume that chemical changes are coupled with some physical and structural rearrangements within the amorphous aluminosilicate particles. It is difficult to imagine such reorganization without a partial dissolution of the solid and at least short transport via the solution. Therefore, during the induction period, a gradual transformation of the gel takes place, which includes changing of Si−O−Al bond angles and short-range transport of (alumino)silicate species. Thus, the chemical evolution of the system is closely related with structural transformation of the gel network. The depolymerization of the aluminosilicate network is most probably induced by the nuclei formed during the mixing of the reactants. However, this process is extremely slow under ambient conditions, which explains the long induction period observed in the present study. Such a nucleation/crystal growth mechanism was observed during the formation of LTA-type under ambient conditions from a TMA-containing system.[37] Growth by propagation through the gel network of isolated nuclei was observed in the formation of LTL-type zeolite by Tsapatsis et al.[46] For the system under investigation, this mechanism dominated during the induction period, where progressive evolution of the composition of the gel particles was observed without change in their morphology. As stated above, the chemical and structural evolutions of the system are two features of the induction process leading to more open network and intense exchange of species between the solid and liquid parts of the system. Thus, the transformation of some part of the initial material, 10−15% according to the XRD data, into zeolite induces the onset of crystal growth (after 11−12 days of treatment). During the period of crystal growth, the aggregation around a crystallization center became the dominant crystallization mechanism. The TEM investigation showed that

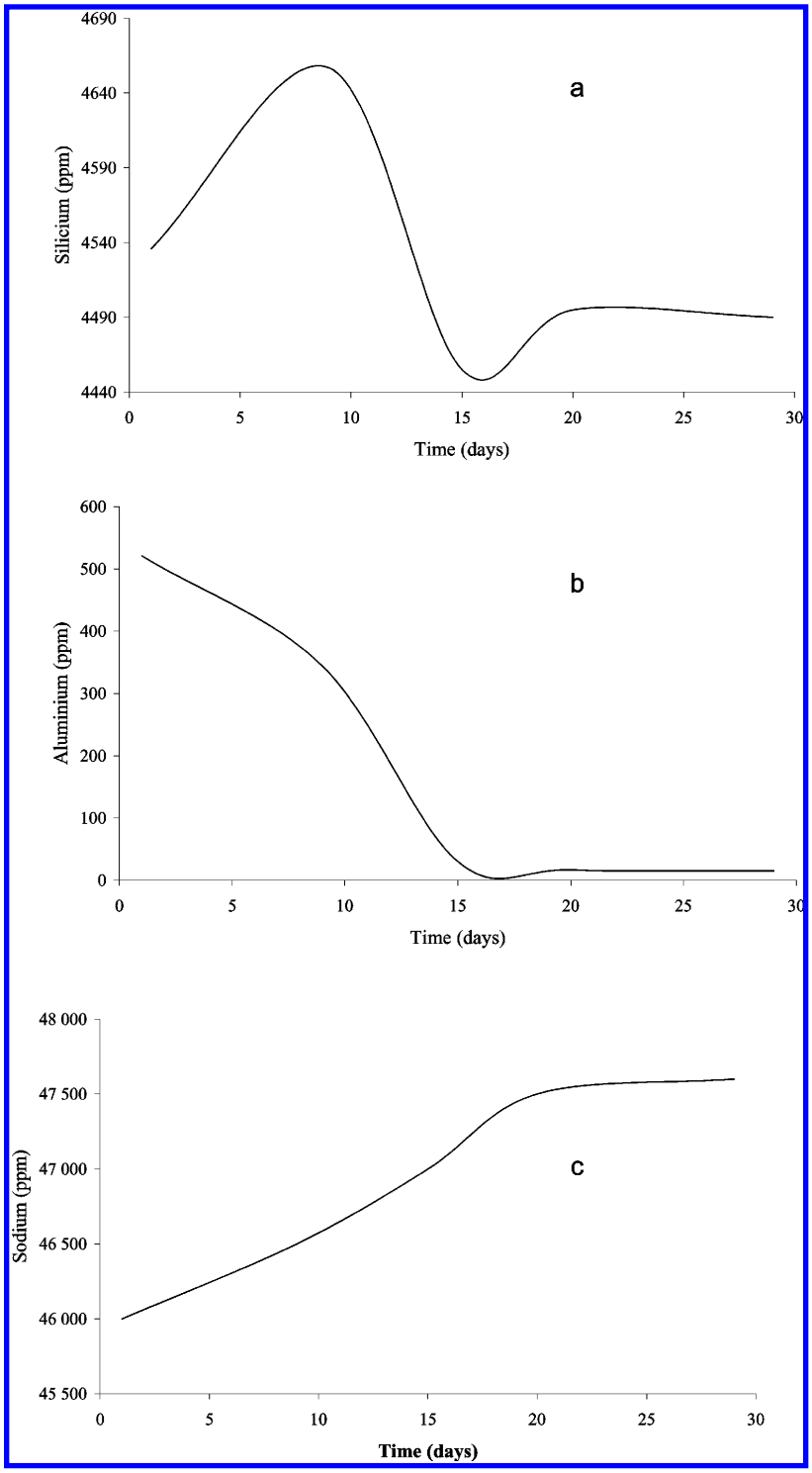

Figure 10. Dissolved silicon (a), aluminum (b), and sodium (c) concentrations of the liquid phase obtained from zeolite X synthesis gels as a function of aging time.

in the course of zeolite crystallization, rounded aggregates of fairly uniform size were formed. The particles building the aggregates were individual crystals with the expected lattice fringes of the FAU-type zeolite [for example (111) (Figure 8)]. The morphological features of the aggregates suggest a crystal growth process that takes place around one crystallization center for each aggregate.

Aggregation of pre-organized similar in size (4 × 4 × 1.3 nm) nanoslabs with the MFI topology was described by Kirschhock et al.[47] According to this group, the MFI-type crystallizes by self-organization of nanoslabs containing pins and holes.[48] The pins are provided by the tetrapropylammonium (TPA) cation protruding out of the three faces of each nanoslabs, whereas the holes are the micropore openings on the opposite side. Thus the crystal growth requires a perfect alignment of the nanoslabs so that the pins match the holes. We have also observed aggregation of preformed particles around a crystallization center. However, the particles in the system under investigation differ substantially in size. In addition, we did not observe any alignment of the crystalline particles forming the aggregates. Alignment in some parts of the aggregates was observed at a later stage when the growth was controlled by the Ostwald ripening. In addition to these observations, the crystallization mechanism suggested for silicalite-1 (MFI-type

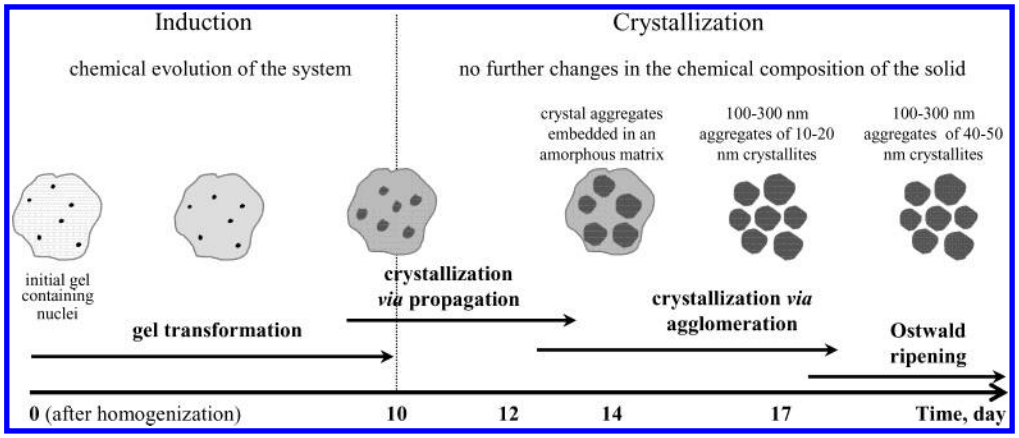

Figure 11. Schematic illustration of the crystallization mechanism of FAU-type zeolite under ambient conditions.

framework) requires an organic structure directing agent (TPA) and therefore cannot be applied for the organic-free gel system, utilized in the present study.

A schematic presentation of the events taking place during the formation of FAU-type zeolite at room temperature is shown in Figure 11. The interpretation of the TEM data is in favor of a crystallization mechanism wherein the beginning stage includes progressive chemical evolution coupled with structural transformation of the initial gel. The changes in the gel system are induced by nuclei of FAU-type structure formed inside the gel during the homogenization of the reactants. This process, where growth by propagation through the gel network dominates, takes about 10 days. After this induction period the gel aggregates collapse and fast, almost instant crystallization takes place around individual crystallization centers. During the period of 14 to 17 days of crystallization most of the amorphous gel is transformed to crystalline particles, which form spherical aggregates with small crystals (10−20 nm in size) in the center and larger crystals in the periphery. The large crystals are a consequence of growth induced by the direct contact with the solution, which facilitated faster diffusion rates and improved supply of nutrients. It is possible that the relatively uniform size of the crystalline aggregates is induced by the chemical potential gradient, which is created during the spontaneous mass crystallization. It could be speculated that such a gradient would induce further crystal growth in the volume closely surrounding the sites of spontaneous mass crystallization. If the newly attached particles are amorphous, the crystal growth in these particles might be promoted by the interface between the particles. This process continues until the nutrient pool, i.e., the amorphous aluminosilicate gel, is totally exhausted. In the system under investigation this process occurred over the 11−22 day period, as the crystallization rate is very high between the 14th and 17th days. The well-shaped crystals with developed crystal faces suggest a solution mediated transport of nutrients during this stage (Figure 8d,f).

The particles continue to grow after 22 days. At that stage, however, the nutrients are provided by the dissolution of the smaller and less stable zeolite nanoparticles; i.e., the system enters in the Ostwald ripening stage.

Conclusions

An organic-free system was used for the synthesis of a FAU-type zeolite under room-temperature conditions. A well-crystallized material containing 100−300 nm spherical aggregates built of 10−20 nm nanocrystals was obtained after 3 weeks of synthesis. Further aging of the system led to an increase of the size of the crystallites without changing the size of aggregates.

The ambient conditions and slow crystallization kinetics allowed a detailed study of all stages of zeolite formation, from mixing of the reactants to the complete transformation of the gel into a crystalline zeolite-type material followed by an Ostwald ripening of the crystals. The nanometer scale transformations were subjected to a TEM study supported by other characterization techniques. The combined analysis of a system crystallizing under ambient conditions provided new insights in the mechanism of zeolite formation. An extensive exchange of species between the solid and liquid parts of the initial system took place during the induction period. Due to this exchange, the system reached a specific critical level of chemical evolution, where the Si:Al ratio of the amorphous gel is close to that of the FAU zeolite. This level of chemical evolution corresponds to transformation of about 10−15 wt % of amorphous matter into zeolite-type material. A crystal growth by propagation through the gel phase dominated during this period. The mechanism that governed the crystallization process in the system under study was fast spontaneous aggregation of nanoparticles around a crystallization center, followed by crystallization and agglomeration of larger crystals around these centers. Such a mechanism produced 100−300 round-shaped aggregates built of 10−20 nanoparticles in the center and larger crystals at the periphery. In the later stages the small crystals transformed to larger ones.

It is worthwhile to mention that negative crystals and liquid inclusions were found in the volume of the gel particles. The interface between the liquid and solid phases in these areas is quite likely to be the places were the zeolite nucleation takes place.

In conclusion, the room-temperature syntheses are a very useful tool for studying zeolite nucleation/crystallization process. Another advantage of the room-temperature synthesis is the formation of zeolite nanocrystals from organic-free gel systems. This approach for the preparation of zeolite nanoparticles can be applied for a number of zeolite materials.

Acknowledgment. V.P.V. is grateful to the CNRS/DFG bilateral program for financial support.

References and Notes

(1) Breck, D. *Zeolite Molecular Sieves*; John Wiley and Sons: New York, 1974.

(2) Szostak, R. *Handbook of Molecular Sieves*; Van Nostrand Reinhold: New York, 1992.

(3) Barrer, R. M. *Hydrothermal Chemistry of Zeolites*; Academic Press: London, 1982.

(4) Serrano, D. P.; van Grieken, R. *J. Mater. Chem.* **2001**, *11*, 2391−2407.

(5) Shi, J.; Anderson, M. W.; Carr, S. W. *Chem. Mater.* **1996**, *8*, 369−375.
(6) Haouas, M.; Gerardin, C.; Taulelle, F.; Estournes, C.; Loiseau, T.; Ferey, G. *J. Chim. Phys.* **1998**, *95*, 302−309.
(7) Twu, J.; Dutta, P. K.; Kresge, C. T. *Zeolites* **1991**, *11*, 672−679.
(8) Sankar, G.; Wright, P. A.; Natarajan, S.; Thomas, J. M.; Greaves, G. N.; Dent, A. J.; Donson, B. R.; Ramsdale, C. A.; Jones, R. H. *J. Phys. Chem.* **1993**, *97*, 9550−9554.
(9) Iwasaki, A.; Hirata, M.; Kudo, I.; Sano, T.; Sugawara, S. Ito, M.; Watanabe, M. *Zeolites* **1995**, *15*, 308−314.
(10) Twomey, T. A. M.; Mackay, M.; Kuipers, H. P. C. E.; Thompson, R. W. *Zeolites* **1994**, *14*, 162−168.
(11) Schoeman, B. J. *Zeolites* **1997**, *18*, 97−105.
(12) Mintova, S.; Valtchev, V. *Microporous Mesoporous Mater.* **2002**, *55*, 171−179.
(13) Norby, P.; Christensen, A. N.; Hanson, J. C. *Stud. Surf. Sci. Catal.* **1994**, *84*, 179−186.
(14) Norby, P. *J. Am. Chem. Soc.* **1997**, *119*, 5215−5221.
(15) Walton, R. I.; Smith, R. I.; O'Hare, D. *Microporous Mesoporous Mater.* **2001**, *48*, 79−88.
(16) Iton, L. E.; Trouw, F.; Brun, T. O.; Epperson, J. E. *Langmuir* **1992**, *8*, 1045−1048.
(17) Dougherry, L. E.; Iton, L. E.; White, J. W. *Zeolites* **1995**, *15*, 640−649.
(18) Dokter, W. H.; van Garderen, H. F.; Beelen, T. P. M.; van Santen, R. A.; Bras, W. *Angew. Chem., Int. Ed. Engl.* **1995**, *34*, 73−75.
(19) de Moor, P. E. A.; Beelen, T. P. M.; Komanschek, B. U.; van Santen, R. A *Microporous Mesoporous Mater.* **1998**, *21*, 263−269.
(20) Tschernich, R. W. *Zeolites of the World*; Geoscience Press Inc.: Phoenix, 1992.
(21) Sand, L. B.; Sacco, A.; Thompson, R. W.; Dixon, A. G. *Zeolites* **1987**, *7*, 387−392.
(22) Ginter, D. M.; Went, G. T.; Bell, A. T.; Radke, C. J. *Zeolites* **1992**, *12*, 733−741.
(23) Ginter, D. M.; Bell, A. T.; Radke, C. J. *Zeolites* **1992**, *12*, 742−749.
(24) Gora, L.; Streletzky, K.; Thompson, R. W.; Phillies, G. D. J. *Zeolites* **1997**, *18*, 119−131.
(25) Zhdanov, S. P.; Hvochtchev, C. C.; Samulevitch, N. N. *Synthetic Zeolites*; Khimia: Moscow, 1981.
(26) Subotic, B. *Zeolite Synthesis*; ACS Symposium Series No. 398; American Chemical Society: Washington, DC, 1989; pp 110−123.
(27) Subotic, B.; Graovac, A. *Stud. Surf. Sci. Catal.* **1985**, *24*, 199−206.
(28) Thompson, R. W. *Zeolites* **1992**, *12*, 837−840.
(29) Gontier, S.; Gora, L.; Güray, I.; Thompson, R. W. *Zeolies* **1993**, *13*, 414−418.
(30) Wenqin, P.; Ueda, S.; Koizumi, M. *Proc. 7th Int. Zeol. Conf.*, Kodahansha, Tokyo **1986**, 177−184.
(31) Xu, W.; Li, J.;.Li, W.; Zhang, H.; Liang, B. *Zeolites* **1989**, *9*, 468−473.
(32) Thompson, R. W. *Molecular Sieves*; Springer-Verlag: Berlin, 1998; Vol. I, Chapter I, pp 1−33.
(33) Cundy, C. S.; Cox, P. A. *Chem. Rev.* **2003**, *103*, 663−701.
(34) Anderson, M. W.; Agger, J. R.; Thornton, J. T.; Forsyth, N. *Angew. Chem., Int. Ed. Engl.* **1996**, *35*, 1210−1213.
(35) Agger, J. R.; Anderson, M. W.; Pervaiz, N.; Cheetham, A. K. *J. Am. Chem. Soc.* **1998**, *120*, 10754−10759.
(36) Bronic, J.; Subotich, B. *Microporous Mater.* **1995**, *4*, 239−242.
(37) Mintova, S.; Olson, N. H.; Valtchev, V.; Bein, T. *Science* **1999**, *283*, 958−960.
(38) Bozhilov, K. N.; Green, H. W.; Dobrzhinetskaya, L. *Science* **1999**, *284*, 128−132.
(39) Yang, S.; Navrotsky, A.; Phillips, B. L. *Microporous Mesoporous Mater.* **1998**, *46*, 137−151.
(40) Mokievskii, V. A. *Crystal Morphology*; Nedra: Leningrad, 1983.
(41) Givargizov, I. *Growth of Filamentary and Scaly Crystals from Vapor*; Nauka: Moscow, 1977.
(42) Wagner, R. S. *J. Cryst. Growth* **1968**, *3*−*4*, 159−161.
(43) Viti, C.; Frezzotti, M. L. *Lithos* **2001**, *55*, 125−138.
(44) Bonev, I. K.; Kouzmanov, K *Eur. J. Mineral.* **2002,** *14*, 607−620.
(45) Nikolakis, V.; Vlacho, D. G.; Tsapatsis, M. *Microporous Mesoporous Mater.* **1998**, *21*, 337−346.
(46) Tsapatsis, M.; Lovallo, M.; Davis, M. E. *Microporous Mater.* **1996**, *5*, 381−388.
(47) Kirschhock, C. E. A.; Ravishankar, R.; Jacobs, P. A.; Martens, J. A. *J. Phys. Chem. B* **1999**, *103*, 11021−11027.
(48) Kirschhock, C. E. A.; Buschmann, V.; Kremer, S.; Ravishankar, R.; Houssin, C. J. Y.; Mojet, B. I.; van Santen, R. A.; Grobet, P. I.; Jacobs, P. A.; Martens, J. A. *Angew. Chem., Int. Ed.* **2001**, *40*, 2637−2640.